



Fellenius, B.H. and Ruban, T., 2020. Analysis of strain-gage records from a static loading test on a CFA pile. *Journal of the Deep Foundation Institute*, 14(1) 39-44.

# Analysis of strain-gage records from a static loading test on a CFA pile

**Bengt H. Fellenius<sup>1\*</sup> and Tony Ruban<sup>2</sup>**

**Abstract:** A static test was performed on a 610-mm diameter, 10 m long CFA pile installed through 3 m of clay and sand and into a thick deposit of lacustrine clay. The loading procedure included prolonged load-holding and an unloading-reloading event, which adversely affected the interpretations of the strain records and demonstrated the inadvisability of not performing a test with equal load-increments and equal load-holding durations and avoiding all unloading-reloading sequences. The pile was strain-gage instrumented at three levels and the recorded strains were used to calculate the pile axial stiffness and determine the load distributions for the applied load. Back-calculations using effective stress analysis were fitted to strain-gage determined load distributions and were then used in simulating the measured pile-head load-movement of the test pile.

**Keywords:** *static loading test, CFA pile, strain-gage instrumentation, axial stiffness*

## Introduction

In the early geotechnical years, static loading tests often included one or more long load-holding duration followed by an unloading-reloading sequence. It was generally believed that the “net” movement after unloading indicated the pile toe movement for the load applied before the unloading—recognizing that the pile toe movement is a key information of a loading test. Over the past few decades, the geotechnical profession has come to recognize that the unloading-reloading does not provide information on the toe response and that meaningful results of a static loading test requires instrumentation. Unfortunately, the old test procedure is still often the one pursued. The profession has not yet fully recognized that the test schedule of a static loading test on an instrumented pile must apply constant load increments, each held a constant for equal length of time, and that no unloading and reloading sequences should be included. Particularly, an unloading-reloading event will adversely affect the strain records and impair a proper analysis because the associated double reversal of the shear forces along the pile builds in a significant hysteresis effect on the strain records. The presented case history is an illustration of the consequence of the such interruption and serves to caution about intentionally including unloading-reloading events in a static loading test programme. Moreover, the interpretation of

the strain-gage records is not just a matter of multiplying measured strain with an E-modulus and pile area.

## Soil Profile and Test Pile Arrangement

The site is located northeast of Edmonton, Alberta, and comprised about 3 m of loose silty sand overlying a thick deposit of firm to stiff lacustrine clay. The groundwater table was at 1.5 m depth and the natural water contents of the sand and clay till were 20 and 30 %, respectively. The sand relative density condition was loose to compact, and the clay consistency was firm to stiff.

The test pile was a 610-mm diameter 10 m long CFA pile instrumented with a vibrating-wire strain gage pair at three depths (3.26, 6.76, and 9.56 m below ground) and subjected to a head-down test seven days after concrete placement. N.B., the lowest gage level, SGL 1, is uncomfortably close to the pile toe.

The maximum test load was 1,080 kN and the test schedule called for applying a series of 40-kN load increments nominally every 10 minutes. Actual load increments were applied about every 8 to 9 minutes, measuring the induced pile head movements until reaching a maximum movement of 25 mm. The load was applied by use of a manually controlled pump and all measurements of movement and strain were recorded using a data collector. The 800-kN load level was maintained for 1 hour and the pile was then unloaded in four 9-minute steps to 58 kN, whereafter it was reloaded to 800 kN in three steps. After holding 800 kN for 9 minutes, the test continued by applying 40-kN increments every 9 minutes. On increasing the load from 1,040 kN to 1,080 kN, after 1 minute 30 seconds of holding the load, the pile head movement reached the scheduled 25 mm and the test was terminated. Had the load been maintained to the full nine minutes and, in particular, if the test had been continued by adding increments, additional useful information would have been obtained. There was

<sup>1</sup> Consulting Engineer, 2475 Rothesay Avenue, Sidney, BC, V8L 2B9, Canada

<sup>2</sup> Principal, Tetra Tech Canada Inc., 14940 - 123 Avenue, Edmonton, AB T5V 1B4, Canada

\* Corresponding author, email: [bengt@fellenius.net](mailto:bengt@fellenius.net)

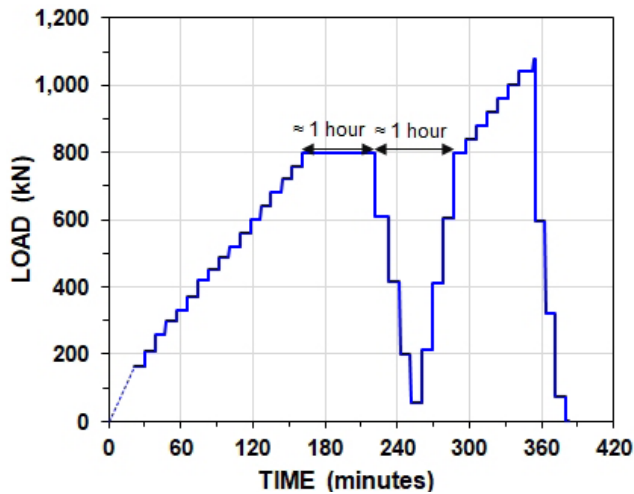


Figure 1. Load-time history

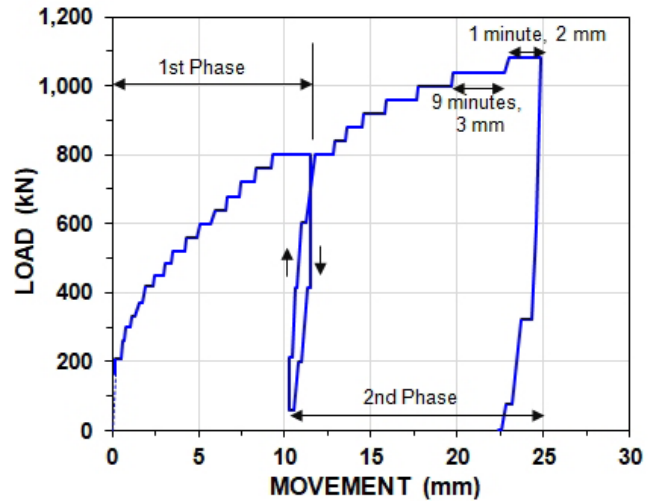


Figure 2. Load-movement history

gage room and time to stay with the scheduled holding time and capacity of the loading system. Figures 1 and 2 show the load-time and load-movement records of the test, respectively. There seem to have been some initial difficulty. Consistent records were only obtained from the start of the fourth load level (166 kN, rather than the 160 kN scheduled).

**Measurement Results**

Figure 3 shows the load versus strain measured at the start and end of each load level for the three gage levels (the levels are numbered from the lowest to the highest and only the records from the fourth load level onward are shown in the load-time and load-movement graphs). The maximum strain measured at SGL 2 is about 40  $\mu\epsilon$ , which is quite small. For detailed analysis, the strain imposed at a gage level should preferably be at least about 300  $\mu\epsilon$  and larger. However, the measured strains are consistent, and the gage pairs indicate that no bending affected the pile. The records are therefore amenable for analysis.

Ordinarily, the load-strain curves should trend to become parallel (and about linear) for loads beyond when the shaft resistance has become fully mobilized between the gage levels. However, as indicated by the straight-line extension of the linear portion of the curves, they are not parallel. This could, of course, be due to the pile cross section being different at the gage levels. However, if so, the extensions of straight line for the gage levels down the pile (SGL 1 and SGL 2) should still cross the ordinate above the origin—the more above, the more shaft resistance between the gage and the pile head. (This notwithstanding that lines derived from records of equal cross sections, thus parallel, from gage levels affected by residual force in the pile will tend to plot lower than from gage levels unaffected by residual force). It is probable that despite the larger movement relative to the soil—larger than 20 mm—the shaft resistance was not been mobilized to a plastic response at gage levels SGL 2 and SGL 1, or the shaft resistance was strain-hardening.

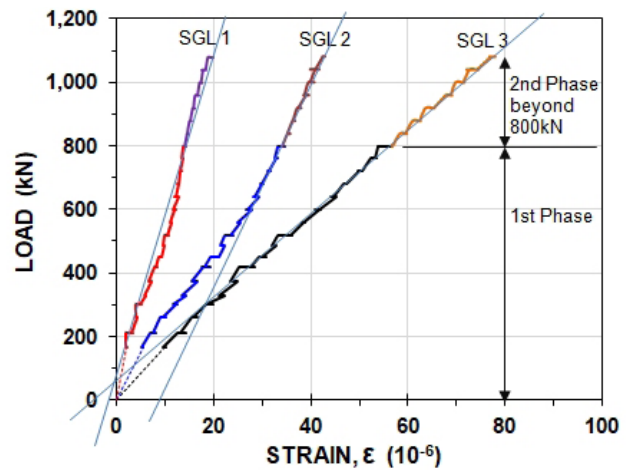


Figure 3. Load-strain records

The slope of the SGL 3, being from a gage level close to the pile head and with minimal influence of shaft resistance and, therefore, having no residual force, represents an approximate value of the pile axial stiffness, EA. In contrast, the slopes of the SGL 1 and SGL 2 curves do not represent the true stiffness of the pile at the gage level. This will be discussed further below.

Determining the pile stiffness from records of axial strain can be performed by the secant-stiffness method (Fellenius 2020). Because this method only applies to gage levels essentially unaffected by shaft resistance from the pile head down to that level, instrumented test piles are for this reason usually supplied with a strain-gage level near the pile head (though not too close, strains are not truly representative of a plane stress surface until about two to three pile diameters below the pile head). The secant-stiffness method consists of plotting all loads, Q, divided by the strain,  $\epsilon$ , versus strain and its veracity depends on the reference to zero strain being accurate. The secant stiffness,  $E_s A_s$ , is the slope of the so-plotted line. The line is only

horizontal for pile material that have constant E-modulus, such as steel piles. Concrete piles normally exhibit a sloping stiffness line due to having an E-modulus that diminishes with increasing stress (and strain). Typically, the low-strain modulus of concrete pile can be about 20 % larger than that at large test loads, which impose strains in the range of 200 to 400  $\mu\epsilon$ . A strain measurement multiplied by its secant-stiffness relation is then the load evaluated from that measurement. Strain records from gage levels affected by shaft resistance, that is, gage levels further down the pile, cannot be analyzed by the secant-stiffness method, but require using the tangent stiffness (incremental stiffness) method (Fellenius 1989; 2020). The tangent stiffness method consists of plotting an increase of load,  $\Delta Q$ , divided by associated increase of strain,  $\Delta\epsilon$ , versus strain. The tangent stiffness,  $E_t A$ , is the slope of the so-plotted line and it slopes twice as much as the secant stiffness line. Thus, the tangent stiffness line establishes the axial secant relation of the test pile.

The tangent-stiffness method is a differentiation method and it is independent of the accuracy of the records' "zero" reading. However, it depends very much on the accuracy of the specific values of load and strain; rather, the accuracy of each increment of applied load and increment of measured strain. The main assumption (sometimes presumption) behind the tangent method is that after full mobilization of the shaft resistance above and at the gage level, the shaft shear is plastic and, thus, each additional increment of load reaches the gage level undiminished by shaft resistance. Once the shaft resistance is fully mobilized, the line is straight, and its slope is equal to the axial tangent stiffness of the pile. If the soil response is not plastic, but strain-softening or strain-hardening, the slope changes. If the soil above the gage level is strain-softening, the load increment,  $\Delta Q$ , reaching the gage level is increased due to the loss of shaft resistance above the gage level. The measured increase of strain will then be larger than for the true quotient,  $\Delta Q/\Delta\epsilon$ , and the slope of the line will trend downward. If the soil instead is strain-hardening above

the gage level, then, the measured increase of strain will be smaller than for the true quotient,  $\Delta Q/\Delta\epsilon$ , and the slope of the line will be steeper; trend toward larger stiffness.

Figure 4 shows that the secant stiffness,  $E_s A$ , determined by linear regression of the Phase 1 strain records of the uppermost gage level, SGL 3 (3.6 m below the pile head), is 13.7 GN (and constant within the rather low range measured in the test). Note however, that the initial part of the secant plot for Phase 1 is curved. This is an indication of imprecise value of "zero" strain in the pile. Not surprising, since even a very small error of the "zero" strain is a rather large portion of the applied load to measured strain in the subject test. Indeed, the secant method is very sensitive to error in the zero reading. For example, adjusting all measured strains by subtracting or adding a mere 2  $\mu\epsilon$ , would induce a huge shift of the initial secant stiffness to 16 and 12 GN, respectively. Thus, the ".7" decimal implies an excessive precision not representative of the accuracy of the stiffness value.

The Phase 2 secant-stiffness plot shows an unacceptable slope in reloading before  $60 \times 10^{-6}$  strain surpassing the maximum strain in Phase 1. It is a bit surprising that the secant stiffness from Phase 2 (i.e., that after the recovery from the unloading-reloading event; from records beyond the maximum load of Phase 1) is just about the same as that determined from Phase 1. Usually, the secant stiffness is larger for reloading conditions.

Figure 5 shows the tangent stiffness of all three gage levels. For the uppermost gage level, SGL 3, the tangent stiffness values,  $E_t A$ , for the end of Phases 1 and 2 is about 13.0 GN. However, the tangent-stiffness method for SGL 2, Phase 2, while at first aiming toward a similar response to that of SGL 3, at about 20  $\mu\epsilon$ , it changes to an upward trend. This is consistent with the shaft resistance becoming strain-hardening after full mobilization.

The analysis of strain records will apply an axial pile stiffness,  $EA$ , of 13 GN. For the 610-mm nominal pile diameter, this indicates an E-modulus of 44 GPa, which is a rather large value even for a pile with steel reinforcement, but is

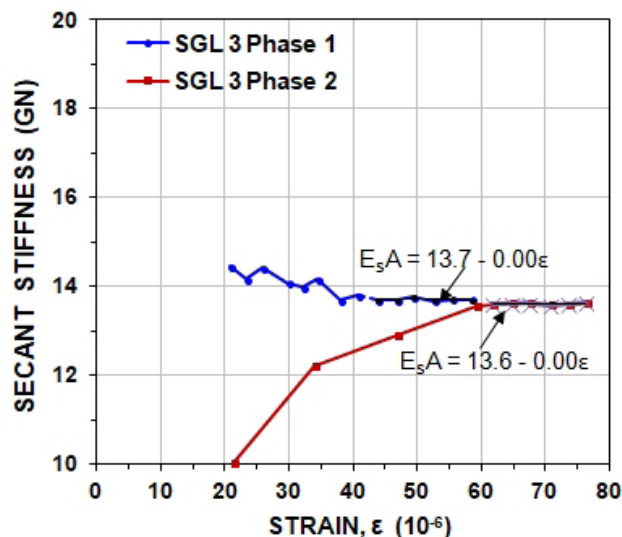


Figure 4. Secant stiffness

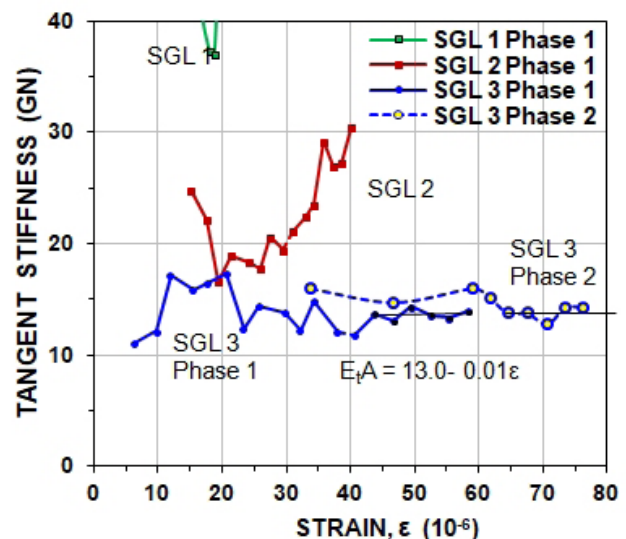


Figure 5. Tangent stiffness

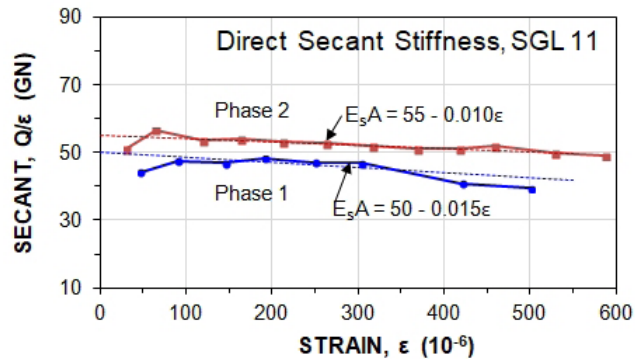


Figure 6. Secant stiffness vs. strain

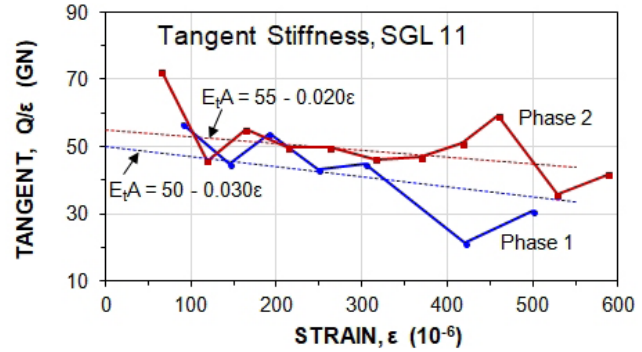


Figure 7. Tangent stiffness vs. strain

probably due to the actual pile diameter being larger than the nominal; a diameter about 50 mm larger than the nominal 610 mm would bring the E-modulus to a more reasonable value. However, the actual pile size and E-modulus are not important as the calculation of the axial force in the pile relies on the stiffness, EA, which is a consistent value determined from the test records.

To additionally illustrate the adverse effect of including an unloading-reloading event in a static loading test, the evaluation of the relatively marginal values of strain measured in the subject case is compared to the similar analysis of a larger pile subjected much larger strains as illustrated in Figures 6 and 7. The records are from a static head-down loading test on a 1,200 mm diameter, 55 m long bored pile constructed in Vietnam (Fellenius and Nguyen 2019). Similar to the subject test, the test scheduled included an unloading-reloading event, Phases 1 and 2. The load-holding duration was 60 minutes and the extra holding time at the end of Phase 1 was 24 hours. Phase 1 comprised loads up to 24.7 MN and Phase 2 up to 34.6 MN, which loads imposed about ten times larger strains than the 800 and 1,040 kN loads in the subject 610-mm pile.

Figure 6 shows the secant stiffness ( $E_s A$ ) of the two phases,  $E_s A = 50 - 0.015\epsilon$ . The figure shows that a secant stiffness line developed also for the reloading phase. However, the stiffness was significantly larger for the reloading phase of the test,  $E_s A = 55 - 0.010\epsilon$ .

As mentioned, the tangent-stiffness method is quite sensitive to small variations of load. Because the loads were applied manually and poorly maintained—the loads recorded are the assigned loads, which probably deviated somewhat from the actually applied loads—the tangent stiffness numbers from both Phases 1 and 2 show a considerable scatter of values. The scatter does not allow determining the tangent-stiffness lines of either phase. An approximate comparison between the methods is indicated by adding to the figure the secant stiffness lines converted to tangent stiffness lines (by doubling the  $\epsilon$ -coefficient).

### Load Distribution

The strains measured at the three gage levels, SGL 1, SGL 2, and SGL 3, were multiplied with a 13-GN axial pile stiff-

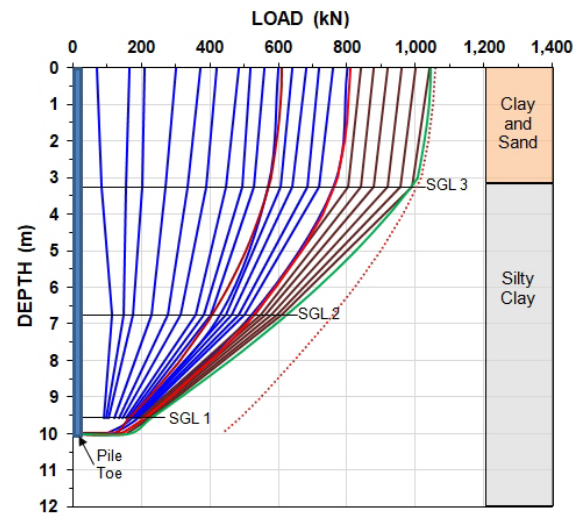


Figure 8. Load distribution for the applied loads

Table 1. Analysis parameters

Depth (m)	$\sigma'$	600 kN		800 kN		1,040 kN	
		$\beta$	$r_s$	$\beta$	$r_s$	$\beta$	$r_s$
	(kPa)	(-)	(kPa)	(-)	(kPa)	(-)	(kPa)
MOVEMENT	(mm)		5		10		20
0.0	0	0.20	0	0.24	0	0.24	0
3.00	48.0	0.20	9.6	0.24	10.6	0.24	11.5
3.00	48.0	0.30	14.4	0.45	21.6	0.84	40.3
3.26 (SGL 3)	50.6	0.31	15.6	0.46	23.1	0.84	42.2
6.76 (SGL 1)	85.6	0.41	34.9	0.56	47.7	0.77	65.5
9.56 (SGL 1)	113.2	0.49	55.4	0.64	72.4	0.71	80.5
10.0	118.0	0.50	59.0	0.65	76.7	0.70	82.6
10.0 (Toe)	118.0		400( $r_t$ )		500( $r_t$ )		550( $r_t$ )

ness to obtain the load generate at the respective gage level for each load applied to the pile head. Figure 8 shows the loads plotted in a load distribution diagram. The pile toe load was estimated by extrapolating the curves. The diagram also shows distributions at 600, 800, and 1,040 kN target loads

back-calculated in an effective stress analysis. The figure includes the pile-head load-movement curve for reference.

Table 1 presents the effective stress parameters,  $\beta$  and corresponding unit shaft shear ( $r_s$ ), that fitted the measured distributions at the 600, 800, and 1,040 kN target loads. The movement for the applied load is also listed in the table. Although the increase of shaft resistance with depth became less pronounced with increasing load, there is no indication of it becoming smaller with increasing load and movement. In fact, the back-calculation indicated that the clay is slightly strain-hardening

### Simulation of Load-Movement Curve

The measured pile-head load-distribution can be simulated in an analysis, modeling the soil response by applying t-z functions (q-z for the pile toe response). Such functions are based on simple stress-movement relations where the input is the shaft shear in percent of a target value determined in a back-calculation from a strain-gage level coupled with the movement measured for the target load. A pile can be considered composed of a series of short elements, each with a soil response described by a t-z function and the specific load and movement of the gage level. When combined with a series of loads applied to the pile head, the pile head movement can be calculated for each load to show a simulated load-movement diagram. The calculations are made by trial-and-error efforts that are simple enough for being carried out in a spreadsheet—although this effort would be very time-consuming. The simulations of the current case were performed using the UniPile5 software (Goudreault and Fellenius 2014).

Figure 9 shows the measured and simulated curves each fitted to the measured curve and movement at three points on the test curve: the end-of-load-level readings for the 600-kN and 800 kN load levels of Phase 1 and the 1,040 kN load level of Phase 2.

Figure 10 shows the t-z and q-z functions applied to 1.0-m pile elements in the simulations for the three target loads (600, 800, and 1,040 kN). The same functions were used for all three analyses.

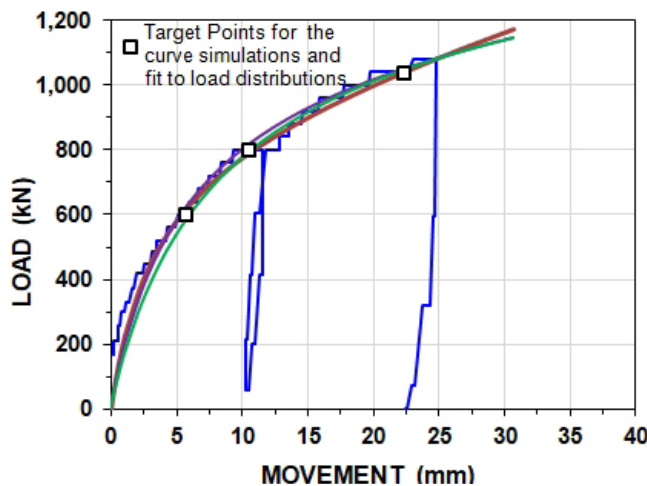


Figure 9. Measured and simulated pile-head load-movement curves

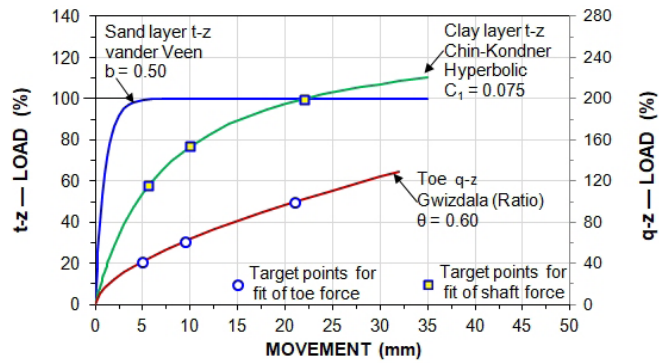


Figure 10. T-z and q-z curves employed in fitting of load-movement response

The back-calculations and simulations established the load-movement response of the pile and the so-calibrated calculation parameters can now be employed in calculations of a similar pile, be it shorter or longer, wider or thinner, with a range of working loads to establish the probable settlement of a foundation supported on the pile or a group. If a static loading test is carried out on an instrumented pile, particularly if without unloading-reloading events and by not varying load-holding duration, while maintaining accurate control of the applied loading, the test results can be used to determine the extent of foundation settlement and an optimum of safe working load. The approach does not preclude also assessing a pile by means of a safety factor applied to a “capacity” defined one way or another, but it allows for a much more confident decision of the expected pile response as a foundation member.

### Conclusions

The unloading-reloading event has affected the evaluation of the pile axial stiffness and demonstrated the desirability of performing a static loading test on an instrumented pile is a single series of load increments, with same load-holding duration for all load levels. The analysis of the strain records enabled the pile axial stiffness and the load distributions to be determined, which were used in simulating the static pile-head load-movement curve. The knowledge of the pile load-movement response with depth makes the results of the test applicable to other slightly different piles at the project site in a much more reliable way than if the test had been used to assess a capacity from the pile-head load-movement curve and deciding on a working load from applying a factor of safety to the capacity value.

### References

Fellenius, B.H. (1989). Tangent modulus of piles determined from strain data. *Foundation Congress*, ASCE, Geotechnical Engineering Division, F.H. Kulhawy, Editor, Vol. 1, pp. 500-510.

Fellenius, B.H. (2016). An Excel template crib sheet for use with UniPile and UniSettle, retrieved from: [www.Fellenius.net](http://www.Fellenius.net).

Fellenius, B.H. (2020). Basics of foundation design—a textbook. Electronic Edition, [www.Fellenius.net](http://www.Fellenius.net), 524 p.

Fellenius, B.H. and Nguyen, B.N., (2019). Common mistakes in static loading-test procedures and result analyses. *Geotechnical Engineering Journal of the SEAGS & AGSSEA*, September 2019, 50(3) 20-31, retrieved from <https://www.fellenius.net/papers/395%20>

Goudreault, P.A. and Fellenius, B.H. (2014). UniPile Version 5 User and Examples Manual. UniSoft Geotechnical Solutions Ltd.